

Extended Range Particle Size Distribution Using Laser Diffraction Technology: A New Perspective

Ted J. Griffin, Jr.: Petrophysical Properties, Inc.

Abstract

Grain size distribution has been traditionally characterized in the oil and gas industry using sieve analysis, settling tube analysis and thin section petrography. These techniques are relatively time consuming and more importantly, do not permit detailed classification of the silt and clay size fractions. Existing laser optics technology developed initially for the powder industry is mature, reliable and can be readily adapted to size distribution analysis of friable and unconsolidated sediments. The measurement range is sufficiently broad, the size determination is rapid and the data are reproducible. The laser optics data compare favorably with sieve analysis and settling tube analysis over traditional measurement ranges and the clay size fraction typically compares favorably with clay content determined by x-ray diffraction.

The extended range data can offer improved insight into well completion strategies, sedimentology, log evaluation and core analysis. From a well completion perspective, both sand and potentially mobile fines can be quantified. The application of the data in sedimentology to determine sediment uniformity can be enhanced since the entire distribution is typically measured. This permits accurate computation of Folk and moment sorting parameters. Also, the measurement range is such that classification of "soft" shales is practical. In addition to these typical applications of particle size distribution, the data have utility in log evaluation. The extended measurements range provides for rapid determination of V_{shale} on cores. Permeability values on percussion-style sidewall cores, typically determined by visual estimation, can be significantly improved with laser optics data.

Introduction

Particle size distribution is important in reservoir evaluation, reservoir geology and well completion. These data have a variety of applications including: (1) engineering application in well completion for gravel pack design¹, (2) geological application in assessing sand heterogeneity and as an aid in depositional environment interpretation², and (3) petrophysical application in formation evaluation to effect an understanding of log responses and to estimate permeability of

percussion-style sidewall cores.

Traditional methods employed to derive particle size distribution data in sands and coarse silts include wet and dry sieving, settling velocity measurements and thin section grain size analysis. The results of these analyses must be combined with the results of hydrometer or pipette analysis to characterize the size distribution throughout the silt and clay size fractions.

Particle size distribution can be readily determined on friable and unconsolidated sands by laser light diffraction. Many diffraction-based instruments exist which utilize the composite diffraction patterns of dispersed particles to compute size distribution. The measurement ranges are broad and are typically inclusive of coarse sand through and including the clay size fractions. Table 1 illustrates approximate measurement ranges for traditional methods and laser diffraction devices. The laser diffraction measurements are rapid, and the resultant data are precise and reproducible.

Instrumentation

The laser device used in the experimentation presented in this paper is a Leeds & Northrup standard range particle size analyzer. The device consists of a sample recirculating system, an optics module and a microcomputer. Figure 1 is a schematic representation of the device. The sample recirculating system comprises a sample receptacle and mixing chamber referred to as a carrier fluid reservoir, a flow loop and a displacement pump that is utilized to suspend the particles and to recirculate the

particle/carrier fluid mixture between the carrier fluid reservoir and the optics module. The optics module contains a solid state laser which generates a 5 mW, 750 nm wavelength beam, all optical components, a glass sample cell (laser window) and an optical detector (photodetector array) for analyzing the diffracted light flux. See Figure 2. The microcomputer serves as the primary operator interface, manages data acquisition, performs calculations, manages data storage and retrieval and performs graphical and tabular report generation.

Size Distribution Measurement

A representative sample is selected (typically 0.4 - 1.0 gram). Sample preparation consists of: (1) extraction and drying to remove hydrocarbons, water and extraction solvent, (2) careful disaggregation with a "soft" mortar and pestle to reduce the sample to individual grains without crushing grains or artificially creating fines, and (3) sonification in a deflocculant solution to disperse particles.

Pre-measurement requirements include verification of laser beam alignment, photodetector array calibration and verification of low level carrier fluid background. The measurement phase is initiated by charging the carrier fluid reservoir with sufficient sample to make a statistically representative determination, but insufficient to create secondary diffraction. The sample is mixed within the carrier fluid reservoir by recirculation and a stream of dispersed particles is displaced continuously through the laser window for analysis. The laser beam is projected through the stream of particles and light is diffracted. A lens transforms the angular distribution of diffracted light to a spatial distribution in the lens focal plane. The resulting spatial intensity is measured by the photodetector array such that the system output is proportional to particle volume. Measurement time is approximately thirty seconds. The time-averaged diffraction pattern shape is a convolution of the

contributions of all of the particles of the composite sample. Signals from the measurement windows are deconvolved into a multichannel histogram of the particle size distribution by a complex algorithm³. Channel progression is set to coincide with sieve screen equivalents. The algorithms used to calculate particle size distribution from composite diffraction patterns are manufacturer dependent and proprietary. However, the following equations can be utilized to illustrate the relationship between the angular extent of the diffraction pattern to particle size and scattered light intensity to particle quantity⁴.

The angular extent of the diffraction pattern is given by:

$$\text{Sine } \theta = (1.22)L/d$$

where:

θ = half angle to the first minimum of the pattern

L = incident light wavelength, microns

d = particle diameter, microns

The total intensity of the scattered light is given by:

$$I = kn d^2$$

where:

I = total diffracted light, watts

K = instrument calibration constant, watts/micron²

n = number of particles

d = particle diameter, microns

It can be observed from these relationships that the angle through which light is diffracted is inversely related to particle size and the diffracted light intensity is directly related to particle quantity.

An example data set in extended sieve analysis format in both tabular and graphical form is found in Figure 3. The sample

percentages within each channel (or retained on equivalent sieve screens) are found in the tabular data in the column labeled "SEP" (or separate) and the cumulative percentages are found in the column labeled "CUM". Particle sizes are provided in phi units ($\phi = -\log_2 \cdot \text{diameter, mm}$), inches and millimeters for the entire data set and equivalent U.S. sieve mesh sizes are also given for the size range over which this comparison is practical.

The graphical display includes separate and cumulative data in both phi units and millimeters. The cumulative curve is scaled to the Y1 axis, and the separate curve is scaled to the Y2 axis. Cumulative percentiles commonly utilized in gravel pack evaluation and sedimentology are indicated in the margin near the Y2 axis; and a legend for the X axis in sand, silt and clay size fraction nomenclature is provided at the top of the graph for reference ease.

Reproducibility and Comparison to Other Methods

Data from two reproducibility experiments are illustrated in Figures 4 and 5. In one experiment, the size distribution for a typical, minimally consolidated Gulf Coast sand sample was determined five times while the sample was recirculating in the flow loop. These data are illustrated in Figure 4 and demonstrate the precision of the determinations. In the second experiment, a sample was prepared and split into five companion samples. The size distribution was determined on each of the samples and the resultant data are illustrated in Figure 5. These data illustrate good reproducibility and are indicative of the expected variation of "split" runs of the same sample if appropriate laboratory technique is employed.

Comparisons of laser diffraction particle size distribution to sieve analysis and to settling velocity tests were made to investigate measurement method bias on naturally occurring samples. The sieve analysis

measurement is such that the minimum grain dimension is determined. The settling velocity test results in equivalent sedimentation diameters (the diameters of spheres of equal densities having equal settling velocities); and the laser data represent the average particle dimension. In theory, these determinations of size would produce the same results if the particles were spherical.

Comparisons of laser diffraction particle size distribution to dry sieve analysis on two samples identified as Test 1 and Test 2 are reported in graphical form in Figure 6 and Figure 7. In the case of Test 1, the two methods compare favorably from .044 mm to .35 mm. In the size fraction $> .35$ mm, the laser diffraction sizes exceed sieve sizes. This difference is the result of measurement bias due to grain shape. Under microscopic examination it was observed that the grains $> .35$ mm in diameter were elongate. In addition to this difference, fines $< .044$ mm were undetected by dry sieve analysis. In the case of Test 2, the methods compare favorably with the exception of the shape bias observed above .35 mm.

A comparison of a twenty minute settling velocity test to laser diffraction is illustrated in Figure 8. Generally the data compare well, although coarser grains and fine-to-very fine silt were observed in the settling velocity test.

It should be noted that in all comparative cases, the sands were medium-to-fine grain and clean. In shaly sands, laser diffraction provides more representative data. In these sands, very fine silt and clay size particle retention on small mesh screens is inherently problematic to dry sieving, as is fines "fallout" from previous runs to the settling velocity technique. In addition, the silt and clay size fractions can be readily classified by laser diffraction.

Comparisons of Clay Content by Laser Diffraction to X-ray diffraction

Comparisons of clay content determination by laser diffraction vs. x-ray diffraction were made to illustrate typical correlations on Gulf Coast sands. These comparisons were undertaken since the clay size fraction is available as a standard component of the laser diffraction particle size distribution. The results are shown graphically in Figure 9. Three sample sets from different Gulf Coast fields are included.

These data indicate that clay content can be estimated by laser diffraction which offers the possibility that the data can be utilized as a selective screening aid for x-ray diffraction analysis. Although clay typing cannot be done rigorously with laser diffraction, rudimentary surface area vs clay content relationships show promise for a basic form of clay typing.

Applications

In sedimentology, size distribution is utilized as an interpretative aid in depositional environment studies. The data are typically reduced to several key parameters descriptive of the distribution. These parameters include the mean and median grain sizes, the sorting coefficient (which describes the uniformity or dispersion about the mean), the skewness (which describes the distribution symmetry) and the kurtosis (which describes the peakedness of the distribution).

Several graphical methods exist for determination of these values including those developed by Trask, Inman and Folk⁵. The graphical methods require specific cumulative percentages. The dilemma with traditional size distribution methods is that in many cases the entire size range is not classified. This results in an open-ended distribution since measurements below ≈ 0.044 mm are not possible or are impractical. This condition exists in silty and/or shaly sands and silts. As a result, the higher percentages have been estimated to calculate the distribution

parameters. The laser diffraction technique classifies the entire distribution and removes this limitation.

Another method of obtaining the key size distribution parameters is computational rather than graphical, and is referred to as the method of moments. Moment calculations are based on the entire distribution, as compared to the graphical methods that are dependent upon several selected percentages. As a result, it is observed by some that this method provides a more adequate representation than the graphical methods. Since the laser diffraction analysis characterizes the entire distribution, moment calculations can be made routinely.

Petrophysics is another area of interest insofar as applications are concerned. The size data can be used to calculate shale volume (V_{shale}) and/or clay volume (V_{clay}) to aid in log evaluation and to estimate permeability on percussion-style sidewall cores.

A wide variety of interpretive V_{shale} models has evolved to determine formation water saturation in shaly clastic reservoirs⁶. Many log-derived V_{shale} indicators exist. V_{shale} can be calculated from the laser diffraction size distribution to confirm or verify log-derived values. Figure 10 illustrates the size distribution of a Gulf Coast shale sample. The distribution is comprised of both silt and clay and corresponds to a $V_{shale} = 100\%$. This distribution can be normalized and deducted from a sand particle size distribution to calculate V_{shale} . Clay volume (V_{clay}) data are also available from the distribution for this application.

Permeability Estimation

Permeability is typically estimated on percussion-style sidewall cores in the Gulf Coast. Historically, permeability has been determined empirically, either by visual estimation of the predominant grain size and

other textural features (resulting in a subjective, experience dependent value) or by grain size measurement using the settling velocity technique.

Laser diffraction size analysis provides rapid classification of the entire size distribution including the silt and clay size fractions that significantly and adversely impact permeability. This extended measurement range provides additional insight to textural characteristics that can enhance permeability estimation.

A typical correlation is illustrated in Figure 10. Permeability values were determined on plugs prepared from full diameter core material. Particle size distributions were measured on the plugs or an adjacent core material. The size distributions were reduced to dimensionless texture coefficients and these values were plotted versus permeability. Equations and correlation coefficients are given in Figure 11. This relationship is subsequently utilized to estimate permeability of sidewall cores with a reasonable degree of confidence on the basis of size distribution data.

Conclusions

Laser light diffraction provides an enhanced description of the particle size distribution of minimally cemented sands, silts and "soft" shales. The measurements are rapid, typically requiring thirty seconds. The size distribution data are precise, reproducible and compare well to sieve analysis and settling velocity tests. The clay size fraction data compare sufficiently well to x-ray diffraction in Gulf Coast sands to indicate relative clay abundance. Accurate computation of graphical and moment sorting parameters is possible given the extended measurement range. V_{shale} can be calculated for comparison to log-derived values. The textural information derived from the particle size measurements can be correlated with measured permeability data to result in more accurate, reproducible and consistent

permeability estimates.

References

1. Saucier, R. J., "Considerations in Gravel Pack Design," Journal of Petroleum Technology (February, 1974), 205-212.
2. Anderson, J. B., Wolfteich, C., Wright, R. and Cole, M. L., "Determination of Depositional Environments of Sand Bodies Using Vertical Grain-Size Progressions," Trans., Gulf Coast Association of Geological Societies (1982), 565-577.
3. Frock, H. N. and Weiss, E. L., "Particle Size Control Using Light-Scattering Technology," Powder and Bulk Engineering (February, 1988).
4. Weiss, E. L. and Frock, H. N., "Rapid Analysis of Particle Size Distribution by Laser Light Scattering," Powder Technology (1976), 287-293.
5. Blatt, H., Middleton G. and Murray, R., Origin of Sedimentary Rocks, Englewood Cliffs, New Jersey, Prectice-Hall, Inc., 1972, 36.
6. Worthington, P. F., "The Evolution of Shaly-Sand Concepts in Reservoir Evaluation," The Log Analyst (January-February 1985), 23-40.

TABLE 1

| | U. S. STANDARD SIEVE MESH | MILLIMETERS | MICRONS | PHI UNITS | WENTWORTH SIZE CLASS | | |
|--------------------------------------|--|-------------|---------|--------------|---------------------------------------|------------------|------|
| Analyzed by Laser Diffraction | Analyzed by Sieve, Thin Section or Settling Velocity Analysis | 10 | 2.00 | 2000 | -1.00 | ----- | |
| | | 12 | 1.68 | 1680 | -0.75 | | |
| | | 14 | 1.41 | 1410 | -0.50 | Very coarse sand | |
| | | 16 | 1.19 | 1190 | -0.25 | | |
| | | 18 | 1.00 | 1000 | 0.00 | ----- | |
| | | 20 | 0.84 | 840 | 0.25 | | |
| | | 25 | 0.71 | 710 | 0.50 | Coarse sand | |
| | | 30 | 0.59 | 590 | 0.75 | | |
| | | 35 | 0.50 | 500 | 1.00 | ----- | |
| | | 40 | 0.42 | 420 | 1.25 | | |
| | | 45 | 0.35 | 350 | 1.50 | Medium sand | SAND |
| | | 50 | 0.30 | 300 | 1.75 | | |
| | | 60 | 0.25 | 250 | 2.00 | ----- | |
| | | 70 | 0.210 | 210 | 2.25 | | |
| | | 80 | 0.177 | 177 | 2.50 | Fine sand | |
| | 100 | 0.149 | 149 | 2.75 | | | |
| | 120 | 0.125 | 125 | 3.00 | ----- | | |
| | 140 | 0.105 | 105 | 3.25 | | | |
| | 170 | 0.088 | 88 | 3.50 | Very fine sand | | |
| | 200 | 0.074 | 74 | 3.75 | | | |
| | 230 | 0.0625 | 62.5 | 4.00 | ----- | | |
| | 270 | 0.053 | 53 | 4.25 | | | |
| | 325 | 0.044 | 44 | 4.50 | Coarse silt | | |
| | 400 | 0.037 | 37 | 4.75 | | | |
| | 500 | 0.031 | 31 | 5.00 | ----- | | |
| Analyzed by Pipette or Hydrometer | | 0.026 | 26 | 5.25 | | | |
| | | 0.022 | 22 | 5.50 | | | |
| | | 0.019 | 19 | 5.75 | | | |
| | | 0.016 | 16 | 6.00 | Medium, fine and very fine silt | | |
| | | 0.013 | 13 | 6.25 | | | |
| | | 0.011 | 11 | 6.50 | | | |
| | | 0.0093 | 9.3 | 6.75 | | | |
| | | 0.0078 | 7.8 | 7.00 | | | |
| | | 0.0065 | 6.5 | 7.25 | | | |
| | | 0.0055 | 5.5 | 7.50 | | | |
| | | 0.0046 | 4.6 | 7.75 | | | |
| | | 0.0039 | 3.9 | 8.00 | ----- | | |
| | | 0.0033 | 3.3 | 8.25 | | | |
| | | 0.0028 | 2.8 | 8.50 | | | |
| | | 0.0023 | 2.3 | 8.75 | | | |
| | 0.0019 | 1.9 | 9.00 | Clay | | | |
| | 0.0016 | 1.6 | 9.25 | | | | |
| | 0.0014 | 1.4 | 9.50 | | | | |
| | 0.0012 | 1.2 | 9.75 | | | | |
| | 0.0010 | 1 | 10.00 | | | | |
| | | | | | MUD | | |

FIGURE 1

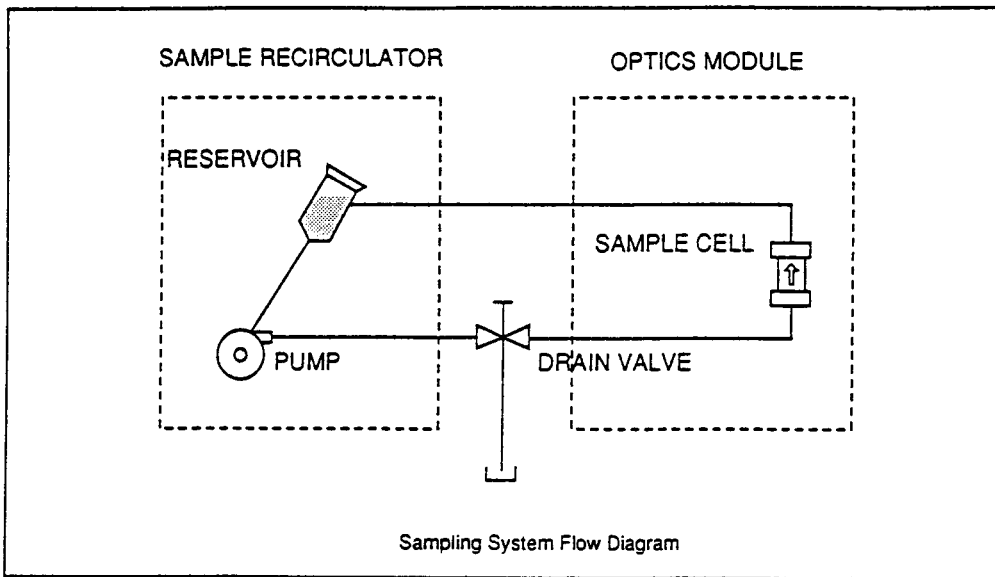


FIGURE 2

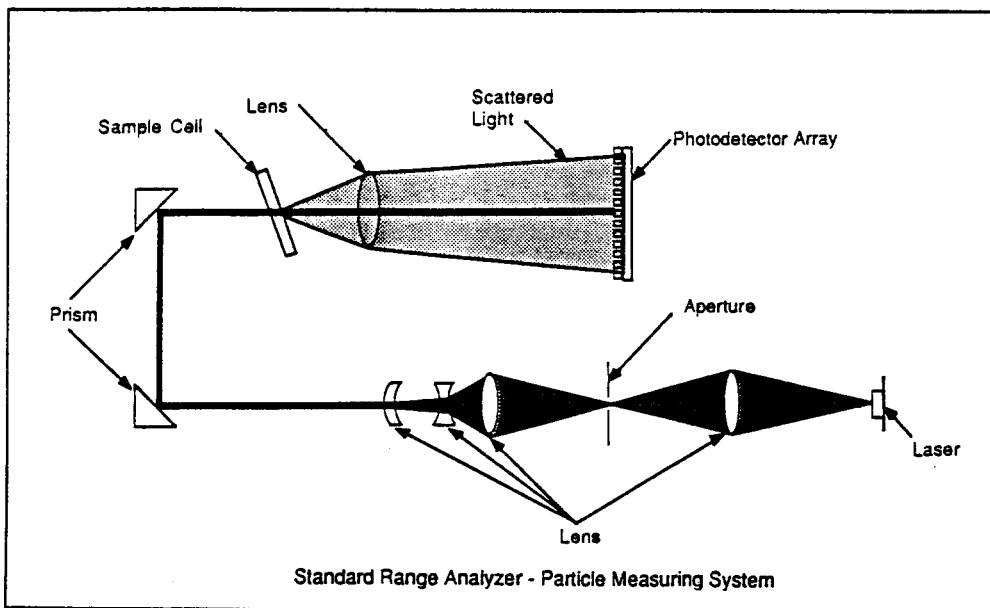
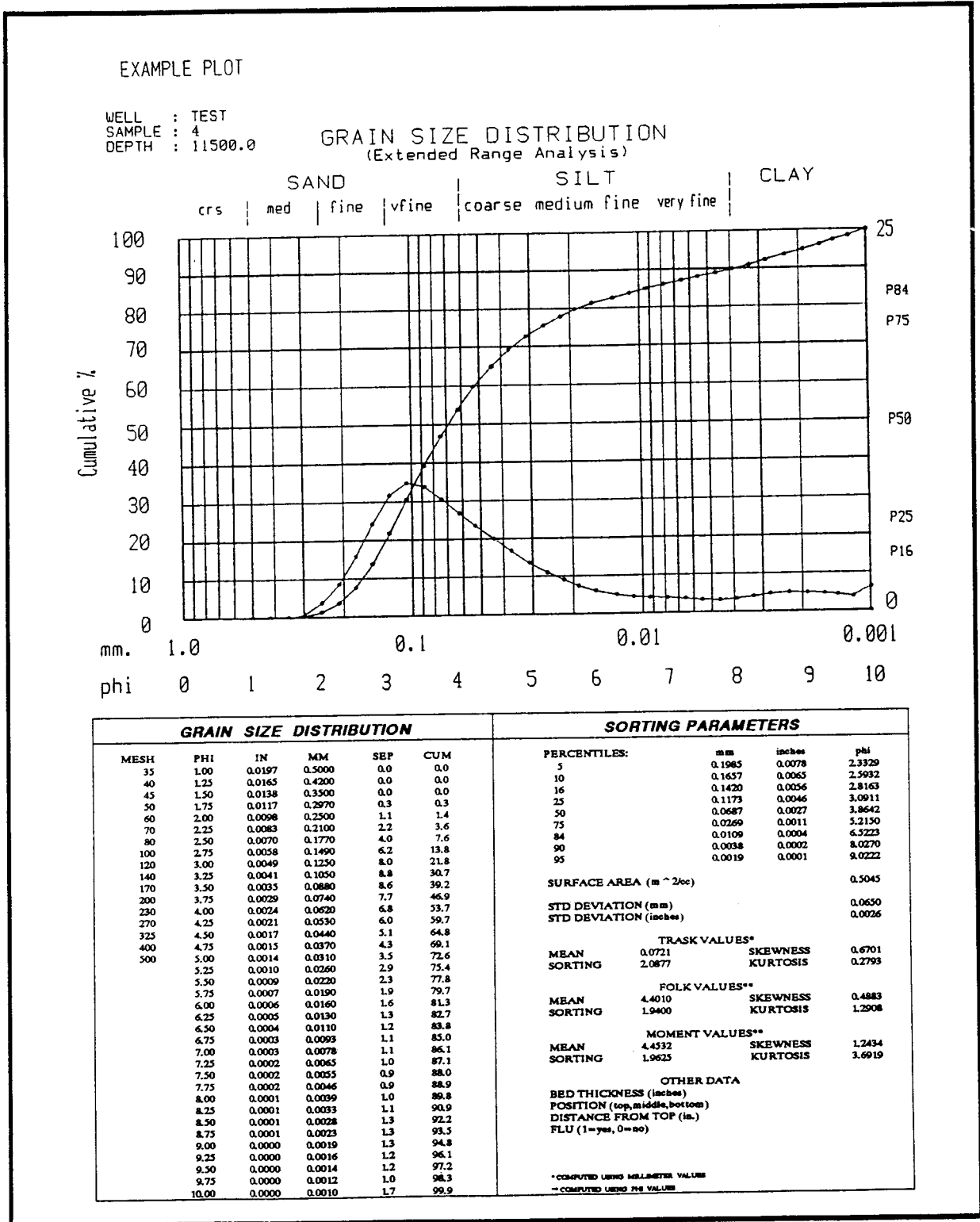


FIGURE 3

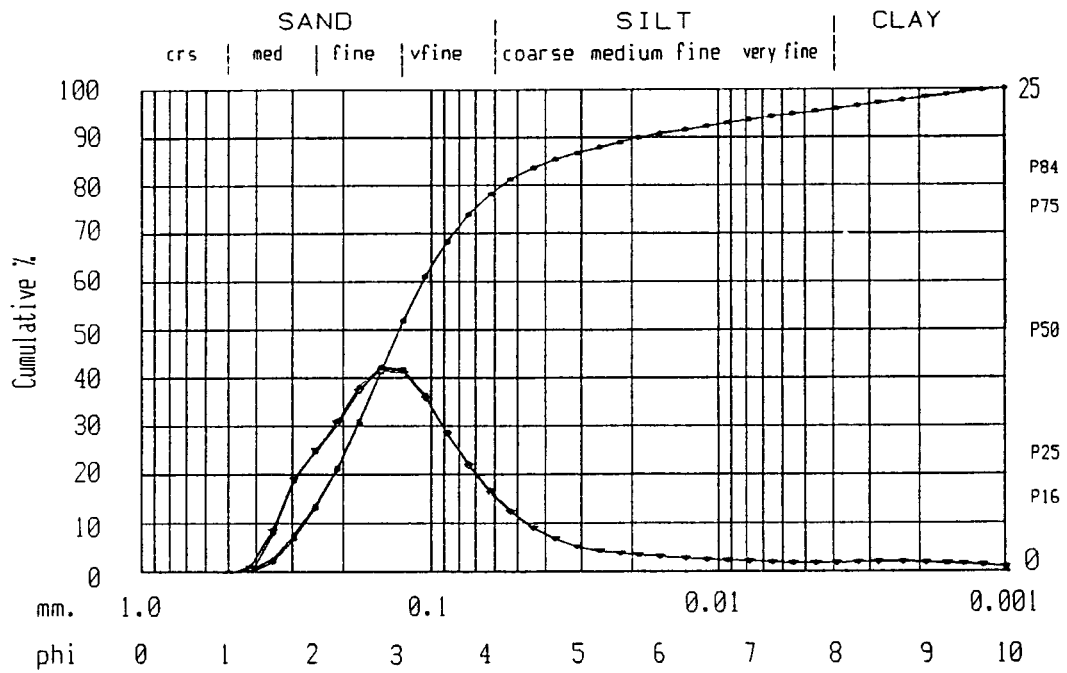


RE-RUN IN LOOP

FIGURE 4

WELL : TEST
 SAMPLE : 1
 DEPTH : 10000.0

GRAIN SIZE DISTRIBUTION
 (Extended Range Analysis)

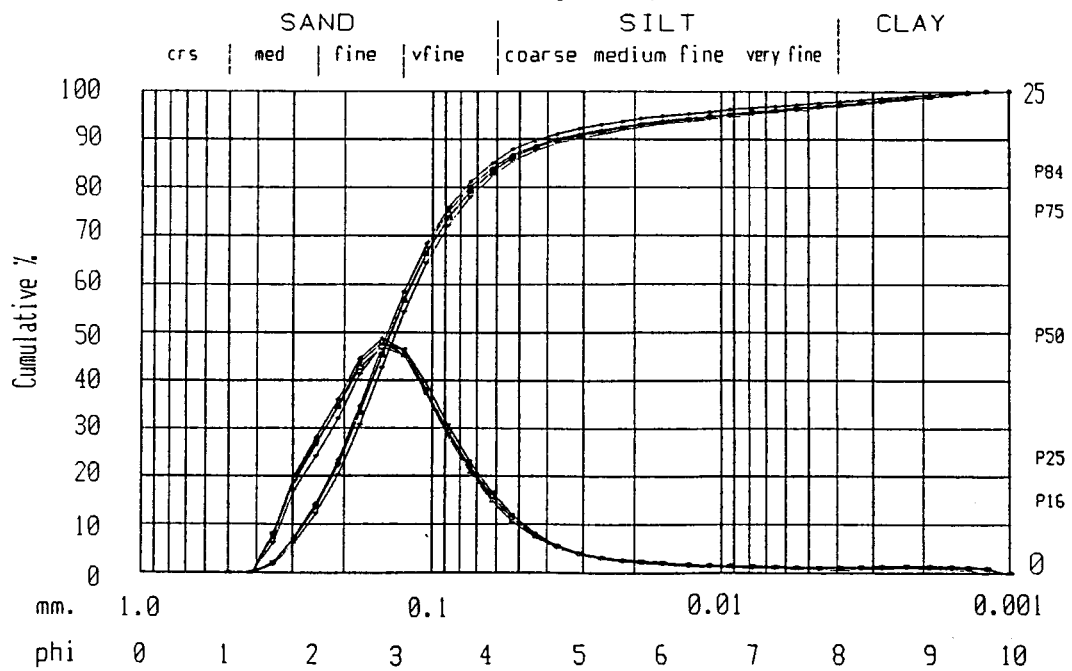


SAMPLE SPLIT RE-RUN

FIGURE 5

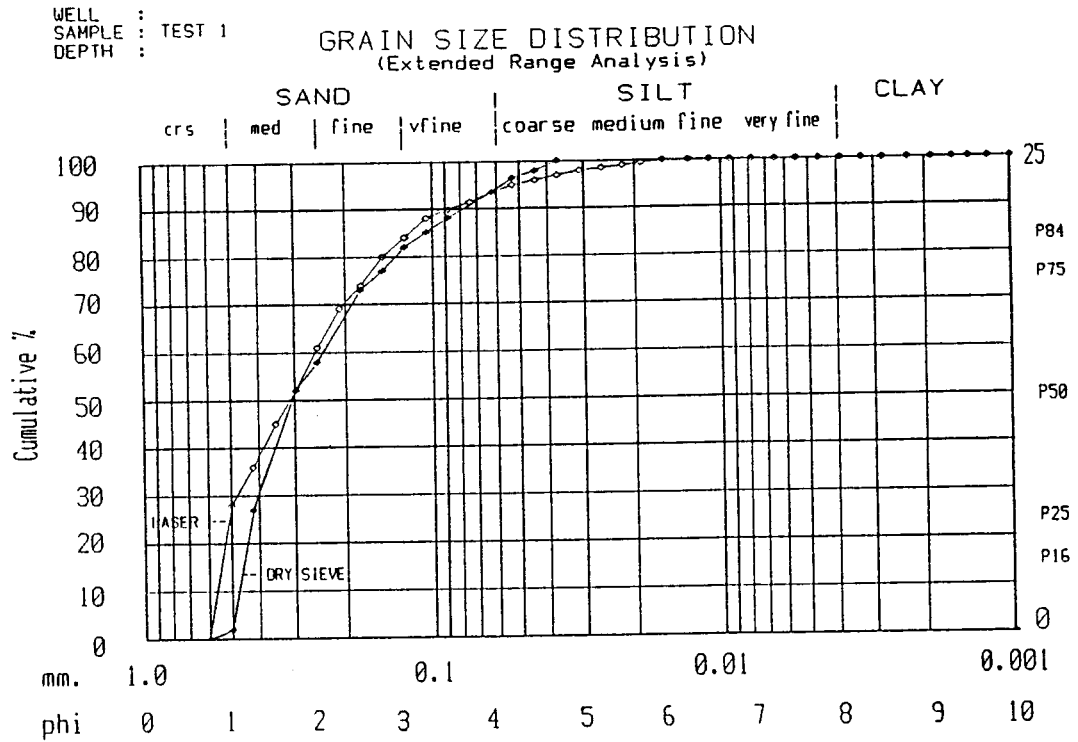
WELL : TEST
 SAMPLE : 2
 DEPTH : 10500.0

GRAIN SIZE DISTRIBUTION
 (Extended Range Analysis)



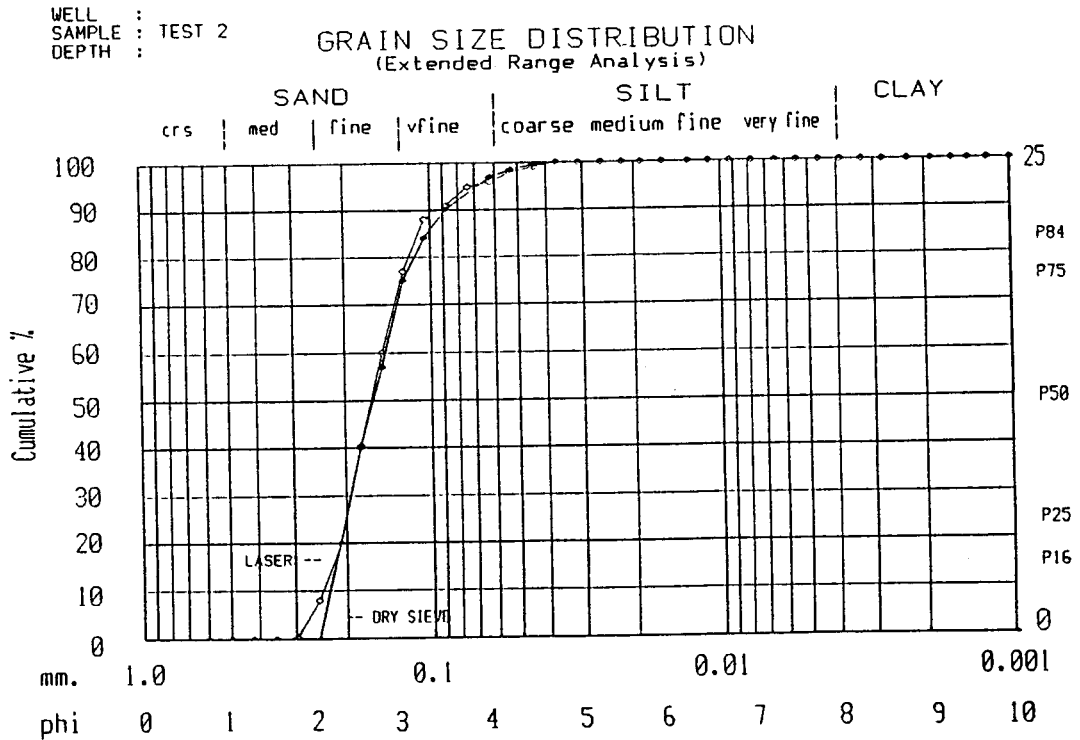
SIEVE COMPARISONS

FIGURE 6



SIEVE COMPARISONS

FIGURE 7



SETTLING COMPARISON

FIGURE 8

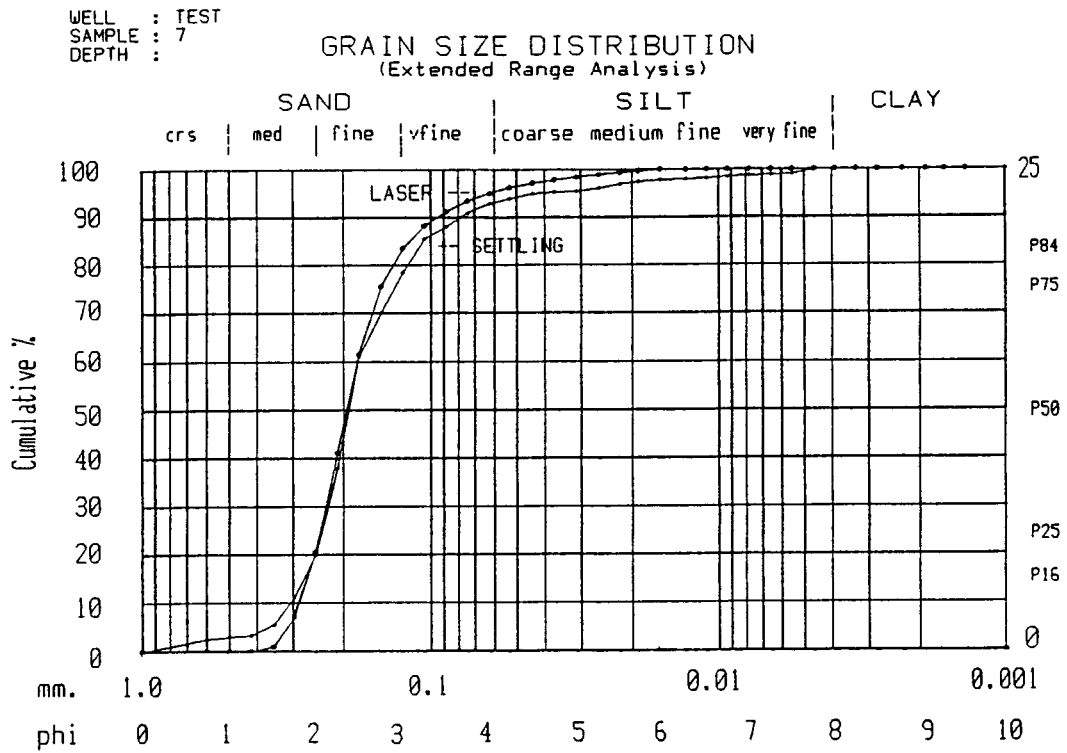
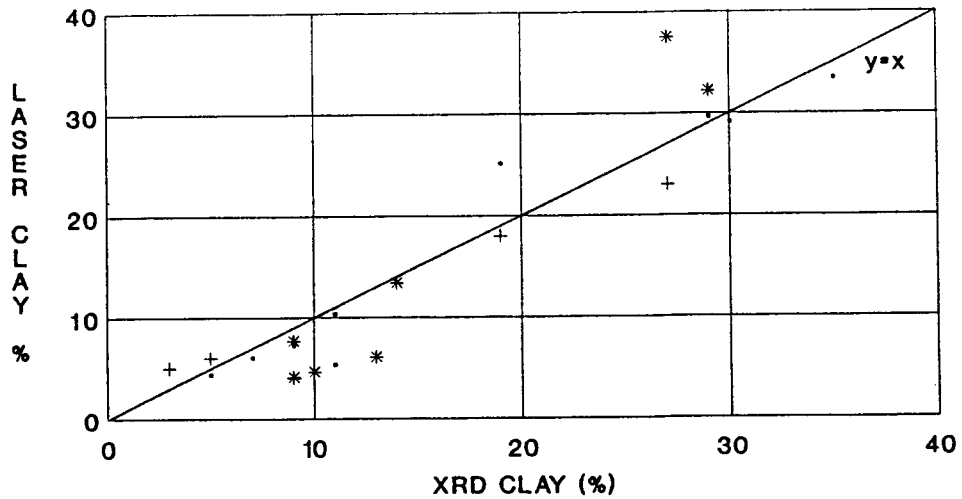


FIGURE 9

CLAY VOLUME COMPARISON
 (xrd vs laser diffraction)



• Data Set 1 + Data Set 2 * Data Set 3

SHALE EXAMPLE

FIGURE 10

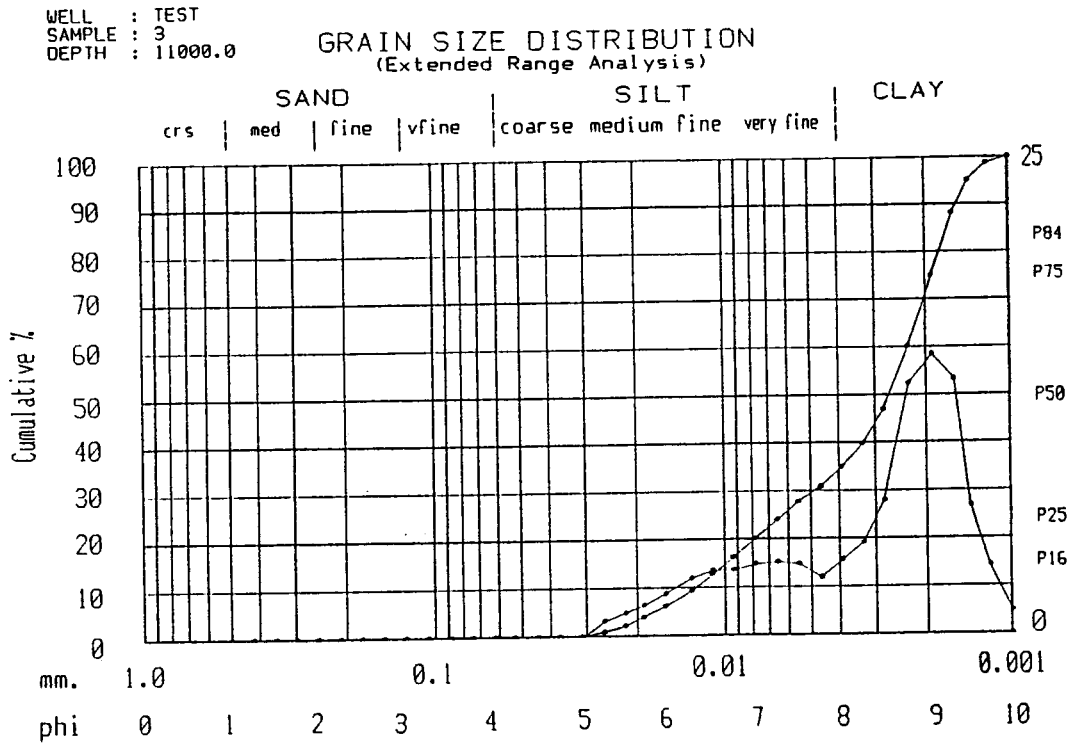
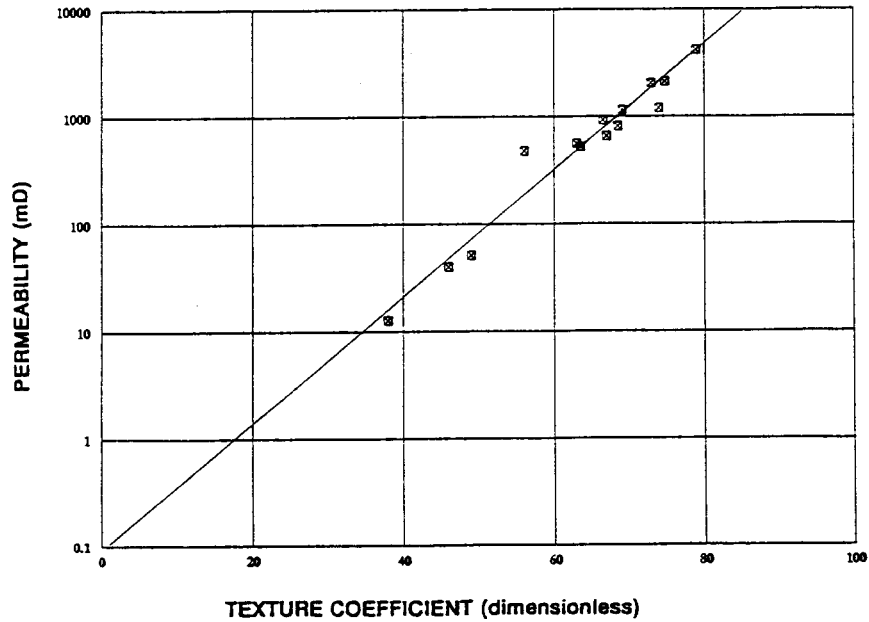


FIGURE 11

PERMEABILITY vs. TEXTURE COEFFICIENT



PERMEABILITY = ANTILOG (0.059 * TEXTURE COEFFICIENT - 1.03)
 CORRELATION COEFFICIENT = 0.955